Environmental Pollution 405 (2026) 128559

Contents lists available at ScienceDirect

Environmental Pollution

journal homepage: www.elsevier.com/locate/envpol

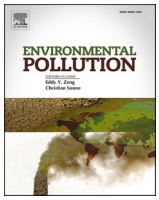

Integrated physicochemical and microbial analyses reveal redox-driven microbial community structure in a polycyclic aromatic hydrocarbon–polluted subsurface

Simon Vandersanden [a,*], Johan van Leeuwen [b], Jaco Vangronsveld [a,c], Sofie Thijs [a]

[a] Environmental Microbiology, Centre for Environmental Sciences, Department of Biology, Faculty of Sciences, Hasselt University, Diepenbeek, Belgium
[b] Utrecht University, Department of Earth Sciences and Water Research Institute KWR, Nieuwegein, the Netherlands
[c] Department of Plant Physiology and Biophysics, Institute of Biological Sciences, Maria Curie-Skłodowska University, Lublin, Poland

ARTICLE INFO

Keywords:
Bioremediation
Polycyclic aromatic hydrocarbons
Electron acceptors
Redox
Soil microbiome

ABSTRACT

Hydrocarbon-polluted sites are a global environmental concern. Although bioremediation is a cost-effective and sustainable remediation method, its efficiency is often impaired by various environmental and microbial factors. Further advancements in bioremediation require a deeper understanding of the relationship between the soil microbiome and the physicochemical parameters that limit biodegradation. Here, we investigated a 3-m-deep polycyclic aromatic hydrocarbon (PAH)-polluted soil core from a historically polluted site in The Netherlands. Soil samples were taken from six depths at 50 cm intervals, followed by a physicochemical characterisation, including measurements of PAH, electron acceptors, pH and electrical conductivity. These analyses were complemented by a detailed microbial community analysis. Our findings suggest that microbial communities are primarily shaped by a combination of the availability of electron acceptors and pollution levels. Additionally, groundwater level fluctuations appear to play an important role in the transport and replenishment of electron acceptors. In-depth community analysis further revealed a diversity of metabolic strategies employed by the different communities to cope with the oversupply of electrons. Collectively, these results demonstrate that microbial communities in PAH-polluted soils vary according to habitat-specific redox environments. Therefore, microbial community analysis can serve as an additional diagnostic tool to infer the specific physicochemical constraints that limit efficient biodegradation. Our findings provide a detailed, integrated interpretation of physicochemical and microbial field data, offering insight into the heterogeneous nature of *in situ* biodegradation. They further highlight the value of comprehensive and integrated microbial community and physicochemical analyses in identifying biodegradation-limiting factors in the field.

1. Introduction

Industrialisation has brought tremendous technological and economic benefits, but it has also left behind disrupted landscapes and polluted soils and (ground-)water. Many current and historical industrial activities have resulted in the accumulation of persistent polluted in soils and sediments. , acting as ticking time bombs from the past. Petroleum-polluted soils can threaten groundwater and aquifers used for drinking water production through leaching and migration, potentially leading to human exposure to hazardous compounds such as polycyclic aromatic hydrocarbons (PAH) (Abdel-Shafy and Mansour, 2016; Falih et al., 2024). Remediation of such sites is essential, however, due to the high costs associated with conventional remediation techniques, many sites rely on passive natural attenuation processes or human-engineered bioremediation as more economical alternatives (Mekonnen et al., 2024; Santos et al., 2025). While these approaches are cost-effective, they are typically slow and governed by complex microbial and biogeochemical interactions (Kour et al., 2021; Mekonnen et al., 2024). Hence, understanding the factors that limit biodegradation is essential for effective risk management and for improving natural recovery potential.

At PAH polluted sites, microorganisms are responsible for the majority of pollutant degradation, alongside abiotic processes (Patel et al., 2020). The efficiency of biodegradation depends on both the metabolic capacity of microbes and environmental constraints (Mekonnen et al., 2024). Aerobic degradation of hydrocarbons is generally efficient,

* Corresponding author. Agoralaan Gebouw D, B-3590, Diepenbeek, Belgium.
E-mail address: simon.vandersanden@uhasselt.be (S. Vandersanden).

https://doi.org/10.1016/j.envpol.2026.128559
Received 19 January 2026; Received in revised form 28 May 2026; Accepted 6 June 2026
Available online 9 June 2026

however it is often limited by the availability of nutrients, pollutant type, pollutant concentration, and other physical parameters (Kebede et al., 2021). Anaerobic degradation is typically slower because it depends on energetically less favourable electron acceptors—such as nitrate, ferric iron, sulphate or carbon dioxide—and often proceeds through syntrophic microbial interactions that enable continued, albeit slow, degradation (Meckenstock et al., 2016; Patel et al., 2020). Microbial communities are shaped by the availability of these electron acceptors and therefore reflect the dominant metabolic strategies and redox state of the environment. Analysing these communities can therefore provide valuable insights into the factors limiting biodegradation and guide targeted interventions to enhance biodegradation.

Various abiotic factors influence PAH degradation rates in soils, such as redox conditions, temperature, pH, nutrient availability, and pollutant concentration (Mekonnen et al., 2024; Patel et al., 2020). Polluted groundwater plumes often develop distinct source and fringe zones, resulting in heterogeneous polluted soils in which biodegradation rates vary spatially and temporally. Source zones are commonly recognized as areas where most dissolved electron acceptors are depleted, and biodegradation is restricted to methanogenesis and the use of insoluble electron acceptors such as iron and manganese oxides (Meckenstock et al., 2015). In contrast. the fringes of the plume may receive a continuous supply of electron acceptors through the inflow of surrounding oxygen, nitrate or sulphate rich groundwater. Groundwater dynamics, including flow conditions and water table fluctuation, play a crucial role in the transport and replenishment of electron acceptors (Meckenstock et al., 2015; Xu et al., 2025). Understanding how these dynamic factors influence the microbial community and degradation potential is essential for predicting and enhancing long-term biodegradation.

At aged sites, such as manufactured gas plants, biodegradation is typically slower due to pollutant adsorption to soil particles, weathering of readily degradable pollutant fractions, and depleted levels favourable electron acceptors such as oxygen and nitrate (Harmsen and Rietra, 2018). Improving natural attenuation strategies therefore requires the identification of factors that limit biodegradation. Distinguishing whether degradation is constrained by substrate availability, electron acceptor availability, or other environmental parameters is essential for implementing low-effort, targeted interventions (Mekonnen et al., 2024). Molecular and metagenomic analyses provide valuable insights into microbial communities; when combined with physicochemical data, they can serve as a diagnostic tool identifying the biodegradation limiting factors (Chettri et al., 2024). The microbial community is a sensitive indicator of environmental stress and can inform the development of strategies to improve *in situ* bioremediation.

In this study, we investigated a 3-m-deep undisturbed soil core from a historically PAH-polluted site in the Netherlands, spanning the unsaturated and saturated zones. Detailed analyses of physicochemical properties and microbial community composition across the heterogeneous layers were conducted to characterize the spatial scale variation in hydrocarbon degrading communities. This comprehensive characterization focuses on community structure, the distinct microbial taxa present at each depth, and how these communities are putatively shaped by environmental conditions. We aimed to determine whether subsurface microbiome structure and functional strategies are driven primarily by hydrocarbon concentrations or constrained by the prevailing redox conditions. The results of this study offer novel insights into microbial assemblages adapting to prevailing redox and substrate gradients. These insights can, in turn, inform the conceptual design and optimisation of bioremediation approaches.

2. Materials and methods

2.1. Site description and soil sampling

2.1.1. Site description and core sampling

Soil samples were collected from a former manufactured gas plant in Utrecht, The Netherlands (SI:1.1 Site description and core sampling) (Faber, 2023). The soil core was extracted using a roto-sonic drill; boreholes are drilled, cored and cased by a rotating and vibrating drill. This resulted in two 15-cm-diameter, 1.5-m soil cores. These were taken from 2.5 to 5.5 m below ground surface (mbgs) at the Griftpark site (52°06′03.0"N 5°07′43.0"E). Together, these two cores formed a 3-m soil core of undisturbed soil containing varying degrees of soil pollution. From the 3 m^1 soil core, six smaller samples were collected at 50 cm intervals to gain an insight into the different layers of the soil core. See SI Section 1.1 (Site Description and Core Sampling) for sample collection details and detailed sample characteristics.

2.1.2. Physiochemical soil analysis

The subsamples from the core was transferred in sterile glass sampling jars and sent for analysis (Agrolab, Al-West, Deventer, The Netherlands). One replicate per SC1-6 samples were analyzed using GC/MS following the methodology described in CMA, section CMA/3/B (OVAM, 2025). Concentrations of pollutants and electron acceptors were reported in $mg.kg^{-1}$ dry soil. To facilitate comparison among samples and to depict the electron acceptors in a biologically meaningful manner, they were converted to the theoretical amount of $mg.kg^{-1}$ benzene which can be oxidized using the available electron acceptors. Calculation details can be found in SI Section 1.2 (Physicochemical soil analysis).

Soil pH and electrical conductivity (EC) were measured from a water extract prepared by mixing fresh soil with deionized water at a 1:2.5 (w/v) ratio and shaking for 30 min. After settling, pH and EC were measured in the supernatant using calibrated meters at room temperature.

2.2. Soil DNA extraction/quality control

From each soilcore sample (SC1-SC6) three biological replicates (separate soil samples of 250 mg soil) was processed, and DNA was extracted using a DNA extraction protocol based on the RNAeasy Powersoil kit (QIAGEN GmbH, Germany). DNA quality assessed using a Nanodrop ND-1000 Spectrophotometer (Isogen Life Science, De Meern, the Netherlands). DNA was quantified using the Qubit dsDNA HS assay kit (Invitrogen) and Qubit 2.0 Fluorometer (Invitrogen). Extracted DNA was stored at −20°C until further analysis.

2.3. High throughput sequencing

Using the Illumina NovaSeq 6000 sequencing platform (2X250), the microbiome was characterized by targeted gene amplification with primers targeting the 16 S rRNA V4 region, and platform specific adaptors and barcodes. NovaSeq library preparation was based on the 515F- improved forward primer (5′-GTGYCAGCMGCCGCGGTAA-3′) and the and the 806R-improved reverse primer (5′-GGACTACNVGGGTWTCTAAT-3′) (read size: 2x250) (Walters et al., 2016).

2.4. Bioinformatic workflow

Demultiplexed raw reads were filtered, trimmed and denoised using Dada2 (Callahan et al., 2016). Then paired end-reads were merged and chimeric sequences were removed. Taxonomic alignment was done using IDTAXA (Murali et al., 2018) against the SILVA 16S rRNA reference database file (version: SILVA_SSU_r138_2_2024). Potential contaminant sequences were identified using the *decontam* R package (Davis et al., 2018) with the prevalence method (threshold = 0.5). Amplicon sequences variants (ASVs) assigned to mitochondria or

chloroplast were filtered out to focus on bacterial sequences for further analysis. All analyses were conducted in RStudio (version 2024.4.1.748) using R (version 4.3.3). Additional details on the bioinformatic workflow and figure generation can be found in SI Section 1.3 (bioinformatic workflow).

3. Results and discussion

3.1. Physicochemical soil description

Initial visual assessments of pollution of the samples (SI Section 2.1: Qualitative soil description) were confirmed by PAH analysis. SC1 (2,5 mbgs) contained 0 mg kg^{-1} PAH, SC2 (3 mbgs) contained 110 mg kg^{-1} PAH, SC3 (3.5 mbgs) 210 mg kg^{-1} PAH, SC4 (4 mbgs) 190 mg kg^{-1} PAH, SC5 (4.5 mbgs) 0 mg kg^{-1} PAH and SC6 (5 mbgs) 23 mg kg^{-1} (Fig. 1A) with raw measurements provided in Supplementary Table 1. The groundwater level was observed at approximately 3.20 mbgs, with average fluctuations of ±0.10 m. Seasonal groundwater level fluctuations are likely higher, due to the presence of mature horse chestnut *(Aesculus hippocastanum)* and European beech *(Fagus sylvatica)* trees, located roughly 3 m away from the sampling point. Examination of PAH concentrations in the different samples reveals the position and structure of the PAH pollution. The source zone is located at about the groundwater table near SC3 (3.5 mbgs) and is flanked by samples SC2 and SC4, which showed lower PAH concentrations. The pH gradually decreased with depth, from 8.85 to 7.86 (Fig. 1A). Electrical conductivity was highest in SC3 (0.149 dS m^{-1}), followed by SC2 (0.123 dS m^{-1}) and SC1 (0.084 dS m^{-1}), with the lowest values observed in samples SC4–SC6 (0.064–0.068 dS m^{-1}) (Fig. 1A).

The relative position of each sample to the groundwater table strongly influenced PAH distribution, with the unsaturated zone (SC2) dominated by heavier 3–4 ring compounds and the saturated zone (SC4) enriched in lighter PAH such as naphthalene (Supplementary Fig. 2). These contrasts reflect differences in volatilization, leaching, groundwater-mediated transport, and biodegradation processes, which collectively modify the PAH profile across saturated and unsaturated

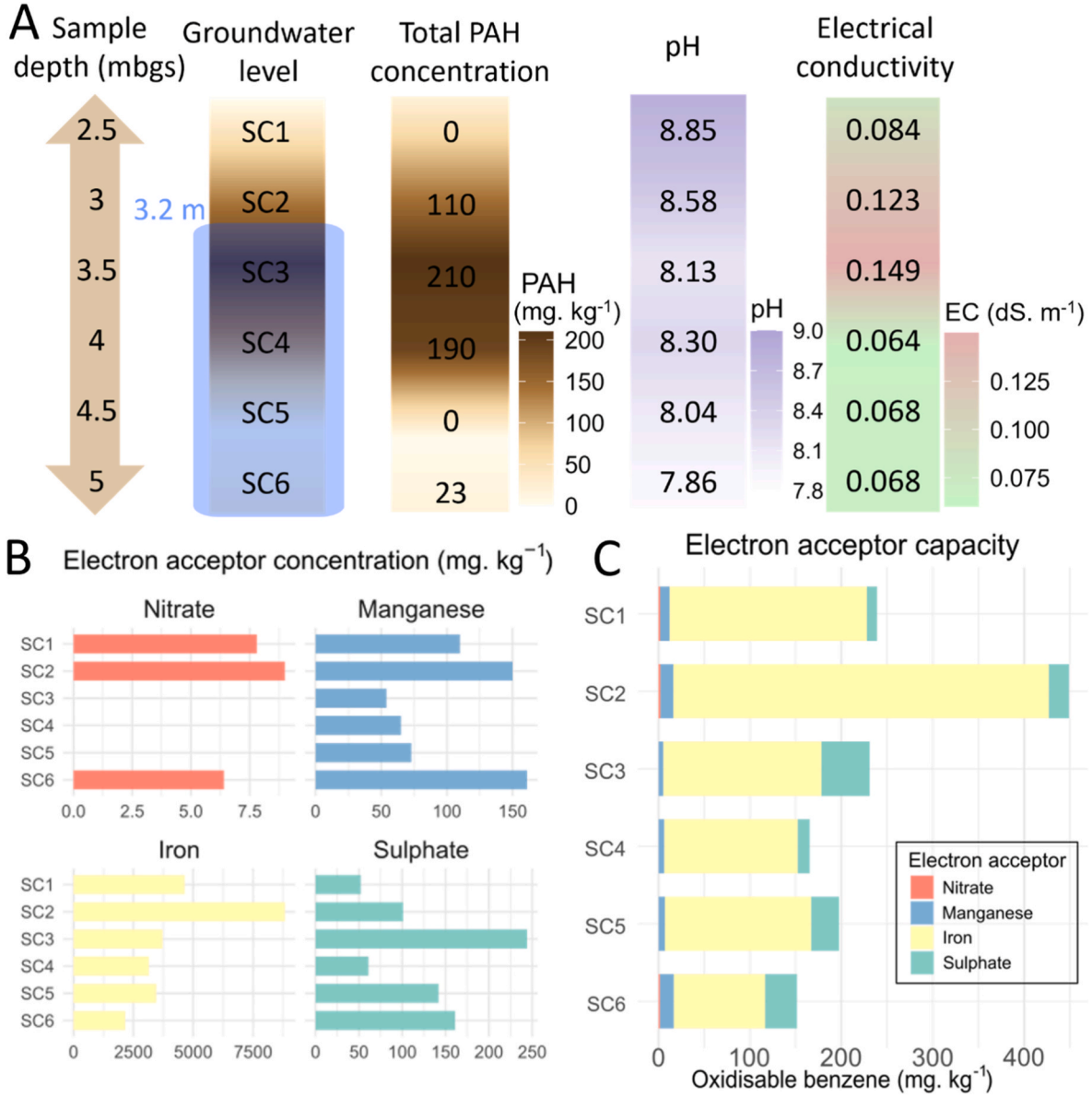

Fig. 1. Physicochemical sample description: (A) physicochemical parameters, sample depth, groundwater level and total PAH, soil pH and electrical conductivity are shown according to the soil profile. (B) Electron acceptor concentrations in soils, shown separately for electron acceptor. (C) Total electron acceptor capacity in the samples, depicted as amount of benzene that could be oxidized using these electron acceptors.

zones. See also 'SI Section 2.2: PAH composition differences', for further information.

3.2. Electron acceptor availability unsaturated zone

Understanding the biodegradation potential in each sample requires consideration of available electron acceptors alongside PAH concentration and composition. An overview of the electron acceptor related soil properties is presented in Fig. 1B. In SC1 and SC2, which are located in the unsaturated zone, nitrate concentrations (7.8 and 9 mg kg^{-1}, respectively), indicate oxic to suboxic conditions. The persistence of nitrate suggests the presence of oxygen, as nitrate would otherwise be rapidly depleted as an electron acceptor by microbes under anoxic conditions (Davis et al., 2009). Moreover, the substantial amount total iron (8830 mg kg^{-1}) found in SC2 likely reflects the oxidation of water-soluble Fe^{2+} to insoluble Fe^{3+} within this layer. Although no unpolluted reference soil was available to account for natural heterogeneity, this observation is consistent with redox-related processes. Iron concentrations in SC2 were markedly higher than in all other samples (2160–4640 mg kg^{-1}) taken form this 3m soil core. Given the position of SC2 relative to the groundwater table fluctuations and PAH pollution, Fe^{3+}-bearing minerals likely act as major electron acceptors for PAH degradation in the saturated zone below SC2, producing soluble Fe^{2+}. This Fe^{2+}-rich groundwater is subsequently oxidized upon upward groundwater fluctuations, precipitating as Fe^{3+} oxides (Xu et al., 2025), leading to the observed total iron enrichment in this layer. Manganese, another mineral-bound electron acceptor, displayed a similar trend, with relatively high concentrations in SC2 (150 mg kg^{-1}) and lower levels in the deeper samples SC3-SC5 (54-73 mg kg^{-1}). Manganese occurs as insoluble Mn^{4+} oxides when oxidized and becomes soluble Mn^{2+} upon reduction. This further supports oxic to suboxic conditions in SC2, and, by extension, in SC1, which was located 0.5 m above SC2.

At this stage of the investigation, it is important to consider the potential role of oxygen. Given sampling depths (2.5-5.5 mbgs), oxygen concentrations are expected to be severely limited due to limited diffusion and consumption of oxygen by plant roots and microbial respiration (Cook and Knight, 2015). Therefore, it is unlikely that oxygen could serve as a major direct electron acceptor in these samples. This is due to its limited electron acceptor capacity at low concentrations, which is similar to what can be observed for nitrate in SC2 (9 mg kg^{-1}) (Fig. 1C). Although energetically favourable, its low concentration restricts its overall electrons acceptor capacity. In contrast, solid-phase electron acceptors, such as iron (8830 mg kg^{-1}) and manganese (150 mg kg^{-1}), represent the majority of the available electron-acceptor potential, even though their energy yields are lower. It is therefore reasonable to conclude that oxygen does not play a dominant role as an electron acceptor in these samples. However, oxygen can still play an indirect role in facilitating biodegradation. Groundwater fluctuations may introduce dissolved oxygen, which microorganisms can periodically use to oxidise and recycle manganese and iron oxides (Anneser et al., 2008; Farnsworth et al., 2012; Xu et al., 2025). Thus, even periodic oxygen inputs reaching these layers can enable a variety of metabolic processes, such as the re-oxidation of solid-phase electron acceptors such as iron and manganese oxides, which subsequently enable multiple pathways for microbial PAH degradation.

3.3. Electron acceptor availability saturated zone

In the polluted samples below the groundwater table (SC3 and SC4), a markedly lower total electron acceptor capacity was observed (Fig. 1C). Soluble electron acceptors such as NO_3^- were absent, and insoluble ones such as iron (SC3: 3720 mg kg^{-1}; SC4: 3150 mg kg^{-1}) and manganese (SC3: 54 mg kg^{-1}; SC4: 64 mg kg^{-1}) were significantly lower than in SC2 (iron: 8830 mg kg^{-1}; manganese: 150 mg kg^{-1}) (Fig. 1B). Lower concentrations of solid-phase electron acceptors, indicate depletion through reductive processes. The manganese concentrations in SC3 and SC4 (54 mg kg^{-1} and 64 mg kg^{-1}, respectively) are close to the solubility limit of MnS (47 mg L^{-1} at 18°C) (9). Total iron remained relatively high (SC3: 3720 mg kg^{-1}; SC4: 3150 mg kg^{-1}), far exceeding the solubility limit of Fe^{2+} typically observed in Dutch aquifers (0-50 mg L^{-1}) (van Beek et al., 2021). However, the iron present is likely poorly accessible, as biological Fe^{3+} oxide reduction slows considerably once reactive surfaces are depleted (Roden, 2003). Consequently, much of the iron present is likely not readily available as an electron acceptor, which is common in zones with high rates of organic matter oxidation where the supply of electrons often exceeds the capacity of Fe^{3+} oxides to uptake them (van Beek et al., 2021). These excess electrons are then diverted toward slower metabolic pathways that yield low energy, such as sulphate reduction, methanogenesis or autotrophic carbon dioxide fixation. Consequently, the oversupply of electrons, restricts biodegradation due to the limited availability of electron acceptors (Meckenstock et al., 2015), often resulting in multiple metabolic strategies occurring within the same layer: Fe^{3+} oxide reduction, sulphate reduction, and methanogenesis (Meckenstock et al., 2015).

SC3 exhibited the highest sulphate concentration (240 mg kg^{-1}), suggesting either sulphate production via sulphur oxidation or limited sulphate utilization das an electron acceptor during PAH oxidation. This may indicate an underdeveloped sulphate-reducing microbial (SRB) community in SC3, as SRB have slow growth rates (doubling time of about ten days) and may struggle to establish in zones with frequent groundwater fluctuations. This is likely due to competition with more energy-efficient microbes (Meckenstock et al., 2015) or to the cycles of growth and death that these SRBs undergo during favourable and unfavourable conditions (Dyksma and Pester, 2024). Though some SRBs genera are aerotolerant, the presence of oxygen remains suboptimal (Demin et al., 2024; Dyksma and Pester, 2024). Given SC3's position relative to the water table, groundwater fluctuations can facilitate transient oxygen influx, potentially delaying or preventing the development of a stable SRB community. In contrast, sulphate concentrations were lower in SC4 (61 mg kg^{-1}) than in the neighbouring samples (142-240 mg.kg-1), suggesting active sulphate reduction. Given the depletion of most electron acceptors in both SC3 and SC4, carbon dioxide likely serves as the dominant terminal electron acceptor.

In SC5, low levels of manganese (73 mg kg^{-1}), iron (3450 mg kg^{-1}), and sulphate (142 mg kg^{-1}) (Fig. 1B) suggest ongoing consumption of these electron acceptors, although not to the same extent as was observed in SC4. This is likely due to SC5 containing only residual PAH concentrations near the detection limit. In SC6, PAH concentrations increased to 23 mg kg^{-1} and were accompanied by higher levels of several electron acceptors. Nitrate (6.4 mg.kg-1) was present, likely due to the inflow of nitrate rich groundwater. Additionally, increased concentrations of manganese (161 mg kg^{-1}) and sulphate (161 mg kg^{-1}) were observed. Total iron concentrations were lower (2160 mg kg^{-1}), possibly due to the outflow of dissolved ferrous iron in the groundwater. Overall, in SC6, several electron acceptors remain limited but available, and are presumably replenished by an inflow of nitrate rich groundwater.

3.4. Microbial community structure

To complement the physicochemical characterization, an in-depth analysis of the microbial communities was done. SC1, SC2 and SC5 exhibited similar community structure and diversity metrics, characterized by high species richness (SR), high Pielou's evenness and low Simpson index (Fig. 2A). In contrast, SC3, SC4 and SC6 shared distinct community traits, displaying low SR, low Pielou's evenness and high Simpson index. As a result, the samples grouped into two general categories: SC1, SC2, and SC5 represented diverse and evenly distributed microbial communities, whereas SC3, SC4, and SC6 were dominated by a few taxa. When these community traits were analyzed in relation to electron acceptor availability, samples with depleted electron acceptors tended to exhibit low SR and low evenness (Fig. 2B). The only exception

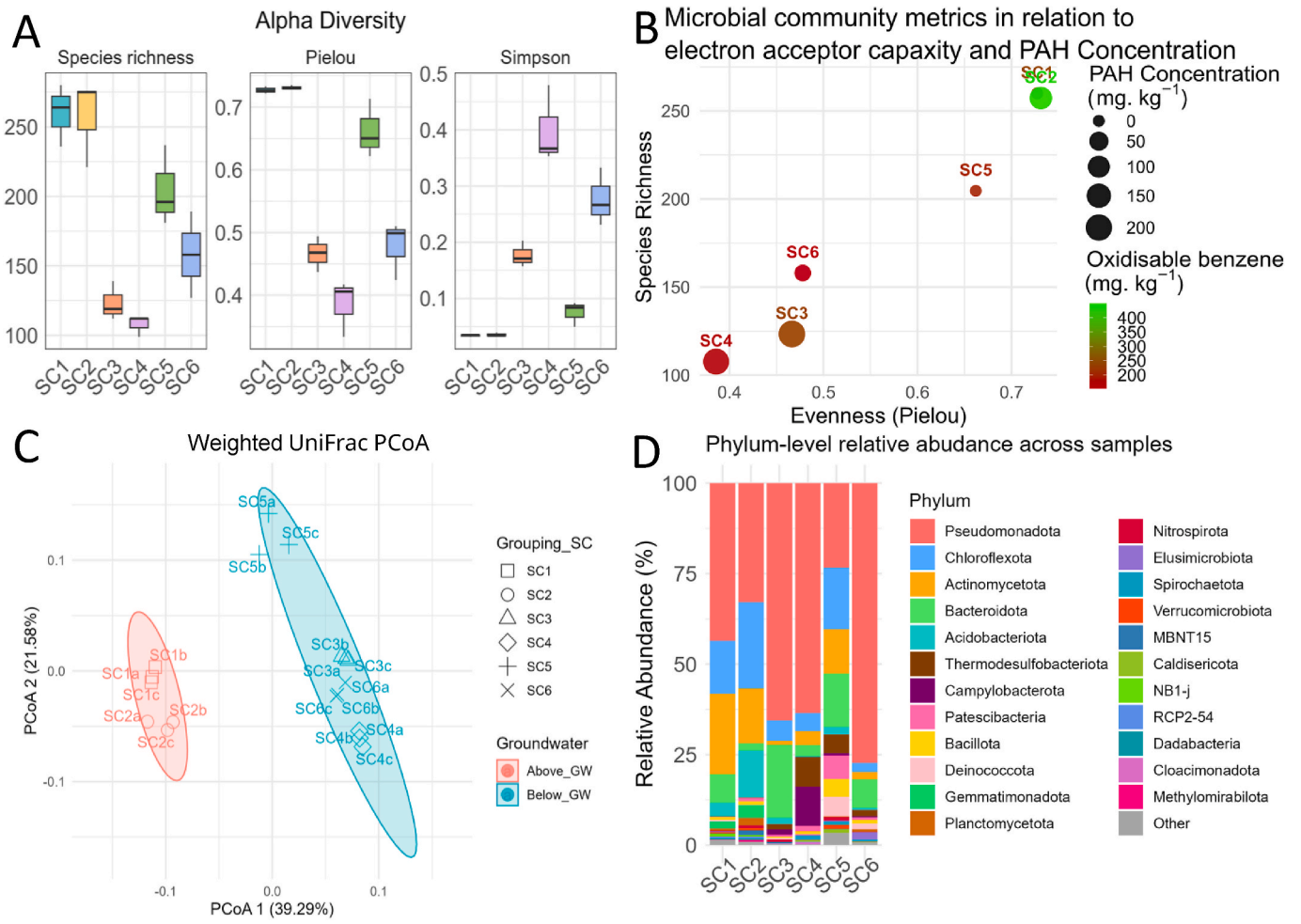

Fig. 2. Overview of the soil microbial community. (A) boxplots showing the different alfa diversity metrics: Species richness, evenness (Pielou's index), Simpson diversity index. (B) Microbial community metrics (Species richness and evenness) in relation to electron acceptor capacity and PAH concentration found in the samples (C) Beta diversity analysis of microbial communities using PCoA based on weighted UniFrac distances (taxa agglomerated on family level) (D) Community composition on phylum level from all samples.

was SC5, which showed limited electron acceptor capacity but high SR and evenness, presumably due to the absence of PAH in this sample. The lack of an excess electron donor supply reduces the competition for available electron acceptors, allowing multiple metabolic strategies to coexist, resulting in a more diverse and balanced community. In SC2, where PAH pollution was detected (110 mg kg^{-1} PAH), the microbial community also displayed high SR and evenness – contrary to the pattern in other polluted samples (SC3, SC4 and SC6) (Fig. 2B). We attribute this to the availability of sufficient electron acceptors, which, similar to SC5, created a balanced redox environment supporting diverse metabolic strategies. These findings suggest that the development of microbial communities in response to PAH pollution depends on both the level of pollution and the availability of electron acceptors.

3.5. *Influence of groundwater level on community structure*

To gain further insight into the overall community structure, a principal coordinates analysis (PCoA) using Weighted UniFrac distances was performed. As shown in Fig. 3C, SC1 and SC2 clustered together on the left side along the PCoA1(39.29%) (Fig. 3C). These are the two samples located above the groundwater table. SC3, SC4 and SC6 clustered together more to the right side along PCoA1; these samples were taken from the saturated zone with pollution and electron acceptor depletion. SC5 is positioned in the middle of PCoA1, but mainly separated along PCoA2 (21.58%). This sample was also located in the saturated zone and thus more electron acceptor limited, but it was not polluted. This ordination pattern indicates that the position relative to groundwater strongly influences the overall community structure.

To statistically validate these observations, a stratified PERMANOVA was performed on the Weighted UniFrac distance matrix (N = 18 total samples; 3 biological replicates across 6 distinct depth profiles). The model evaluated the fixed effects of Groundwater Position, Total PAH concentration, and their interaction term, utilizing a constrained permutation design (999 permutations nested within sampling cores) to eliminate pseudo-replication biases (SI Section 2.3: Community structure ordination statistical analysis). The results indicate a strong trend where groundwater position acts as a primary structuring factor, accounted for 38.4% of the total community variance ($R^2 = 0.384$, F = 12.80, p = 0.069). Notably, this value aligns well with the 39.29% of variance captured by the primary PCoA axis (Fig. 2C), confirming that the horizontal separation of samples is driven primarily by hydrological saturation. Although the p-value was slightly exceeding the 0.05 threshold due to the conservative permutation structure required to account for the nested structure of our samples, the high R^2 value provided a robust quantitative basis for the observed ordination. Furthermore, total PAH concentration and its interaction with groundwater position accounted for an additional 10.5% ($R^2 = 0.1051$, F = 3.51, p = 0.832) and 9.2% ($R^2 = 0.0918$, F = 3.06, p = 0.935) of the community variance, respectively. While these terms do not reach statistical significance within the constrained permutation blocks, their inclusion

allows the overall model to explain nearly 60% of the total microbial community shifts (total model $R^2 = 0.58$). This demonstrates that while hydrological state establishes the overarching ecological baseline across the depth profile, PAH levels operates as a secondary driver of the microbial community.

In the unsaturated zone, the communities are highly similar, suggesting that the presence of PAHs is not the primary driver of community composition. Otherwise, SC1 and SC2 would not cluster so closely together, given the large difference in PAH concentrations between the two 0 vs 110 mg kg^{-1}. In contrast, in the saturated zone, where electron acceptors are largely depleted, the presence and not necessarily concentration of PAH appears to be the main factor shaping community structure, as all polluted samples cluster together, regardless of PAH concentration. The non-polluted saturated zone sample SC5, clearly separates from both the unsaturated zone samples and the polluted saturated zone samples. These observations further refine the observed pollution/electron acceptor dependency pattern, demonstrating that position relative to groundwater plays a major role in microbial community assembly, likely through the replenishment of electron acceptors. Fig. 2D provides an overview of the major phyla, which are discussed the 'SI Section 2.4: Phylum level description', setting the scene for the detailed community analysis.

3.6. In depth description of the microbial community

3.6.1. Above groundwater (clean/polluted)

Focusing on lower taxonomic levels gains deeper insights into specific soil functions or metabolic processes occurring in each layer. However, since 16S rRNA gene sequencing identifies taxonomic presence rather than active metabolic flux, any functional roles assigned to these taxa are interpreted as tentative. These taxa serve primarily as indicators for localized redox conditions or for identifying dominant metabolic strategies. In sample SC1, the microbial community was evenly distributed, with four main families each contributing substantially to the community composition: *Acidimicrobiaceae* (>10%), *Xanthomonadaceae* (>5%), *Acidithiobacillaceae* (>5%) and *Chloroflexota KD4-96* (>5%) (Fig. 3). The *Acidimicrobiaceae* family is associated with the Feammox process, in which ammonium is oxidized under iron-reducing conditions (Huang et al., 2016). *Xanthomonadaceae* includes biosurfactant producing and PAH degrading members (Lu et al., 2019), whereas *Acidithiobacillaceae* are involved in iron and sulphur oxidation (Gleisner et al., 2006; Quatrini and Johnson, 2019). *Chloroflexota KD4-96* are unculturable bacteria which are considered bioindicators of high biological soil health (high respiration and active carbon) (Wilhelm et al., 2023). The order *Burkholderiales* comprised over 10% of the community, with *Massilia* being the most abundant genus (Supplementary Fig. 3). Members of this genus have been linked to aerobic PAH degradation (Wang et al., 2016). Together, taxa with less than 1% relative abundance individually, accounted for over 30% of the total community.

In sample SC2, the dominant families were *Chloroflexota KD4-96* (>10%), *Actinomycetota MB-A2-108* (>5%), *Hydrogenophillaceace* (>5%), *Oxalobacteraceae* (>5%) and unclassified *Vicinamibacterales* (>5%). Both, the *Actinomycetota MB-A2-108* and *Chloroflexota KD4-96* are unculturable bacteria considered as bioindicators of high biological health (high respiration and active carbon) (Wilhelm et al., 2023). Among the *Burkholderiales*, *Hydrogenophilaceae* and *Oxalobacteraceae* were the dominant families, driven primarily by the genera *Thiobacillus* and *Massilia* (Supplementary Fig. 3). *Thiobacillus* species are known for utilizing various inorganic electron donors such as pyrite and other reduced sulphur compounds like (H_2S and S^0) to produce sulphate (SO_4^{2-}); they also oxidise ferrous iron (Fe^{2+}) to ferric iron (Fe^{3+}) (Fortin et al., 1996; Harahuc et al., 2000). *Massilia* species, besides being linked to PAH degradation, have been reported to enhance plant resistance against biotic and abiotic stress and facilitate pollutant uptake in phytoremediation processes (Amirhosseini et al., 2025). *Massilia* was only detected in SC1 and SC2, potentially reflecting its dependence on association with plant roots. Members of *Vicinamibacterales* are aerobic chemoheterotrophs linked to increased phosphorus availability in soils (Huber and Overmann, 2018; Wu et al., 2022; Xia et al., 2023). Phosphorus may represent a limiting factor for microbial growth and PAH biodegradation in SC2. The high pH (8.58) might cause low phosphorus availability, because at these pH ranges phosphorus tends to precipitate with calcium (Hyland, 2006; Penn and Camberato, 2019). Low-abundance (<1%) taxa contributed notably to the community composition, together accounting for over 30% of the total.

Overall, several shared members were observed: *Massilia*, *Xanthomonaceae, Sphingomonadaceae* all of which are all potential PAH degraders. Although PAHs were absent in SC1, the presence of these taxa suggests either that there is a metabolic priming or an inherent potential for PAH degradation if PAHs would be reintroduced through groundwater fluctuations. Nevertheless, clear differences in dominant metabolic strategies emerged between the two samples. In SC1, the community was dominated by several taxa indicative of chemolithotrophic metabolisms (*e.g* Feammox, iron and sulphur oxidation), consistent with the limited availability of organic carbon (PAH) in this sample. In contrast, the community of SC2 shifted toward an organotrophic mode, as reflected by the dominance of *Thiobacillus*. This genus appears to facilitate endogenous electron acceptor production by oxidising reduced species such as Fe^{2+}, H_2S and S^0 into Fe^{3+} and SO_4^{2-}, effectively regenerating the pool of available acceptors for the wider community. The abundance of *Actinomycetota MB-A2-108* and *Chloroflexota KD4-96* indicates elevated respiration and active carbon. The increased relative abundance of phosphate foraging *Vicinamibacterales* suggests that phosphorous availability may be a limiting factor for biodegradation in SC2.

3.6.2. Below groundwater (polluted vs clean)

Given the marked community differences between unsaturated and saturated samples, we discuss the saturated zone samples separately. In sample SC3, the dominant families were *Hydrogenophilaceae* (>10%), *Rhodocyclaceae* (>10%), *Xanthomonadaceae* (>10%) and *Flavobacteriaceae* (>10%). The genus *Thiobacillus* (*Hydrogenophilaceae*), was identified (Supplementary Fig. 3) and likely contributes to electron-acceptor production via sulphate or ferric iron (Harahuc et al., 2000; Quatrini and Johnson, 2019). Its presence may account for the elevated sulphate concentration (240 mg kg^{-1}) observed in this sample. The genus *Rugosibacter* (*Rhodocyclaceae*), are facultative aerobes capable of degrading various PAH (Corteselli et al., 2017b). Additionally, the closely related *Georgfuchsia toluolica and Sulfuritalea hydrogenivorans*, are known as niche specialists capable of the degradation of aromatic compounds under various hypoxic conditions (Sperfeld et al., 2018; Weelink et al., 2009). *Pseudoxanthomonas* (*Xanthomonadaceae*) was identified, a genus known for its potential to degrade PAH and produce biosurfactants (Lu et al., 2019; Sarkar et al., 2016). The genus *Lutibacter* (*Flavobacteriaceae*) also constituted a significant fraction of the community; it possesses an extensive hydrogen metabolism (Kessler et al., 2019). *Lutibacter* can generate hydrogen through hydrogenogenic fermentation, which serves as a temporary electron storage and can accumulate for subsequent utilization by syntrophic partner organisms (Ohmura et al., 1999). Alternatively, under oxygen- or nitrate-rich conditions, hydrogen can be used as an energy source (Kessler et al., 2019) which is notable given SC3's position within the soil. Additionally, the genus Lutibacter has been linked to tolerating in conditions with high $Fe2^+$ (Alharbi et al., 2026). Flavobacteriales are classified as habitat generalists. Genome reconstructions indicate that these taxa are highly metabolically flexible facultative anaerobes that adapt to resource variability by using different electron donors and acceptors (Chen et al., 2021). Low-abundance taxa (<1%) contribute only slightly, accounting for just over 5% of the community.

Sample SC4 was dominated by *Methylophilaceae* (>30%), with notable contributions from *Sulfurspirillaceae* (>5%) and smaller

fractions of *Anaerolineaceae* (>2%), *Geobacteraceae* (>2%), *and Desulfurivibrionaceae* (>2%). *Methylophilaceae* are commonly associated with methanotrophic Bacteria and Archaeae and are specialized in utilizing reduced one-carbon compounds — such as methanol, methylamine and formaldehyde — as sources for energy and carbon (Chistoserdova, 2011; Salcher et al., 2019; Taubert et al., 2019). Their presence in this sample potentially suggest that small amounts of oxygen may have been introduced during sampling, enabling partial oxidation of the methane present in the system, which could have stimulated the growth of *Methylophilaceae*. This would indirectly suggest that methanogenic conditions were prevailing in this soil layer prior to sampling. *Methylophilaceae* have also been linked to the degradation of high-molecular-weight (HMW) PAH (Lu et al., 2019), potentially suggesting that their dominance might also reflect a role in the breakdown of HMW PAH through the metabolism of methylated PAH. Methylated PAH, like HMW PAH, tend to accumulate in older pollution due to their slower biodegradation rates (Chistoserdova, 2011; Mohapatra and Phale, 2021). The presence of *Sulfurospirillaceae* indicates the use of various electron acceptors, such as sulphate, elemental sulphur, or oxygen, for the oxidation of organic acids or hydrogen (Finster et al., 1997; Ross et al., 2016). Which could explain the low sulphate levels in this sample.

Members of the class *Anaerolineaceae* were detected in all saturated zone samples and have been reported in anaerobic sludge fermenters as primary fermenters, providing acetate and hydrogen to methanogens (Bovio-Winkler et al., 2021). Syntrophic interactions between iron-reducing bacteria and members of the *Anaerolineaceae* have been documented during the anaerobic degradation of PAH, with *Anaerolineaceae* as primary PAH degraders. The Fe^{3+}/Fe^{2+} redox couple functions as an electron conduit, facilitating direct interspecies electron transfer and enhancing microbial degradation efficiency of PAH (Lu et al., 2022). The family *Geobacteraceae*, also dominant in SC4, includes taxa that have been reported as members of BTEX degrading consortia in iron reducing conditions (Botton et al., 2007). They are known to be capable of extracellular electron transfer (EET), suggesting that they might act as iron-reducing partners for *Anaerolineaceae* (Weber et al., 2006). *Desulfurivibrionaceae*, a family closely related to *Geobacteraceae*, comprises sulphate- and iron-reducing bacteria that are capable of EET (Chen et al., 2025; Gonzalez et al., 2024). Electrons transferred by these organisms may subsequently be utilized by methanogens through interspecies electron transfer (Su et al., 2023). Given these electron transfer capabilities of *Geobacteraceae* and *Desulfurivibrionaceae* and their close phylogenetic relationship to cable bacteria, which belong to the same phylum (*Thermodesulfobacteriota*) (Kjeldsen et al., 2019; Ley et al., 2024; Pfeffer et al., 2012). It is reasonable to suspect that *Geobacteriaceae* and *Desulfuvibrionaceae* may fulfil roles similar to cable bacteria, including long-distance electron transport towards zones with sufficient electron acceptors. However, as 16S rRNA gene data and phylogenetic relatedness alone cannot confirm active long-distance transport, this remains a suggested conceptual model for electron management in the saturated zone. Low-abundance (<1%) taxa made only a modest contribution to the SC4 community composition, collectively accounting for about 5%.

In the non-polluted sample SC5, the dominant family is *Anaerolineaceae* (>10%), followed by *Weeksellaceae* (>5%), *Burkholderiaceae* (>5%), *Trueperaceae* (>5%), as well as smaller fractions *Syntrophaceae* (>2%), *Bacteroidetes vadin* HA17 (>2%), and *Gallionellaceae* (>2%). The detection of *Anaerolineaceae* in the non-polluted sample SC5 indicates that the community is metabolically primed for hydrocarbon degradation. Which likely reflects an adaptive response to periodic groundwater inflow carrying trace contaminants, maintaining a standing population of degraders in otherwise clean zones. Within the *Weeksellaceae*, the genus *Chryseobacterium* was identified; members of this genus have been associated with crude oil polluted soil and PAH degradation (Márquez-Villa et al., 2023; Oberoi et al., 2015). The *Burkholderiaceae* are known to harbour multiple taxa capable of the degradation of aromatic compounds (Morya et al., 2020; Pimviriyakul et al., 2020). Notably, *Burkholderiaceae* have been observed co-occurring with *Trueperaceae* at the cathode side of microbial fuel cells, highlighting their capacity to deal with a large supply of electrons (Simeon et al., 2022). The relatively high abundance of cable bacteria–related families (*Thermodesulfobacteriota*) in samples SC4 and SC5 may indicate possible electron transfer between the electron-rich SC4 and the more electron-limited SC5 (Kjeldsen et al., 2019). The presence of *Syntrophaceae,* strictly anaerobic microorganisms engaged in syntrophic relationships with methanogens implies that methanogenesis may act as a terminal electron sink in this environment (Walker et al., 2020). This interpretation is supported by the depletion of inorganic electron acceptors, suggesting that the community shifts toward syntrophic associations to maintain thermodynamic viability under highly reduced conditions. *Bacteroidetes vadin* HA17 is a family often found in co-occurrence with methanogens, and are typically found in environments related to complex carbon degradation (Wei et al., 2019). *Gallionellaceae* are primarily known as Fe^{2+} oxidising bacteria, but some members have also been reported to be capable of carbon dioxide fixation. This process may serve as an alternative pathway for electron disposal (Hallbeck and Pedersen, 1991; Huang et al., 2022).

Finally, in sample SC6, the dominant family was *Rhodocyclaceae* (>30%), with other notable contributions from *Hydrogenophilaceae* (>5%), *Weeksellaceae* (>2%), *Bacteroidetes vadin* HA17 (>2%) and *Immundisolibacteraceae* (>2%). At the genus-level, the same dominant genera identified in SC3, *Rugosibacter* (*Rhodocyclaceae*) and *Thiobacillus* (*Hydrogenophilaceae*), were also detected in SC6. This pattern suggests a potential metabolic interaction between these taxa, in which *Rugosibacter* acts as the primary PAH degrader, while *Thiobacillus* functions as a partner organism by generating electron acceptors such as sulphate and ferric iron, thereby facilitating sustained hydrocarbon degradation (Corteselli et al., 2017b; Harahuc et al., 2000; Quatrini and Johnson, 2019). The co-occurrence of these two genera further indicates that SC3 and SC6 share similar geochemical conditions. Both are PAH-polluted saturated-zone samples influenced by periodic inflow of nitrate-rich groundwater and elevated sulphate concentrations. However, SC6 exhibits a greater diversity and abundance of potential electron acceptors (nitrate, manganese, and sulphate) compared to SC3, where sulphate predominates. This further supports the hypothesis that *Rugosibacter* acts as the primary PAH degrader, with *Thiobacillus* supplying or maintaining sufficient electron acceptors. This interpretation is consistent with community composition data: in SC3, *Rugosibacter* and *Thiobacillus* occur in nearly equal proportions, whereas in SC6 (more electron acceptors available) the *Rugosibacter* to *Thiobacillus* ratio increases to approximately 6:1. Additionally, two families, which were also present in SC5, *Weeksellaceae* and *Bacteroidetes vadin* HA17, were detected in SC6. Members of *Weeksellaceae* have been associated with PAH degradation, whereas *Bacteroidetes vadin* HA17 are linked to complex carbon degradation (Márquez-Villa et al., 2023; Oberoi et al., 2015; Wei et al., 2019). *Immundisolibacteraceae* also contributed notably to the community; this family has been reported in literature for degrading high molecular-weight PAH (Corteselli et al., 2017b).

Overall, a general pattern emerges across the saturated zone samples: each sample harbours specific PAH degraders. *Rugosibacter* in combination with *Thiobacillus* appear to be the major PAH degraders in the 'fringe zones', where the redox conditions likely fluctuate periodically due to the inflow of nitrate rich groundwater. Meanwhile, *Anaerolineaceae* are consistently found (>1%) in all saturated zone samples, likely functioning as primary fermenters and hydrocarbon degraders. Depending on the redox conditions, other strains previously linked to PAH degradation were also identified, but usually do not dominate the overall microbial community. Notably, in the PAH polluted samples, many dominant taxa primarily shared a functional trait related to dealing with excess electrons. They often act as iron or sulphate reducers (*Desulfurivibrionaceae, Sulfurospirillaceae*) depending on prevailing redox conditions. In samples where all major electron acceptors were highly

depleted, we observed the presence of various syntrophic microorganisms, or microorganisms capable of carbon fixation (*Syntrophaceae*, *Bacteroidetes vadin* HA17, *Gallionellaceae*). This further strengthens our previously mentioned observation, that the microbial community structure it is not governed solely by the capacity to metabolise PAH but rather the capacity to cope with the overload of electrons derived from the PAHs. The capacity for electron disposal thus appears to be the primary driver of microbial community composition in the saturated zone. Finally, depending on the geochemical conditions, microorganisms appear to employ multiple strategies for electron disposal. Including the use of electron acceptors such as iron oxides, sulphate or interspecies electron transfer with methanogenic or carbon dioxide fixating autotrophs. Additionally, there are some tentative indications that electrons may be transported from electron acceptor depleted zones, potentially mediated by 'cable bacteria' related taxa (*Thermodesulfobacteriota*)(Pfeffer et al., 2012; Su et al., 2023; Walker et al., 2020).

Overall, the composition of the community structures suggests that each community is organised in a way that allows them to manage its specific redox challenges. Table 1 provides a summary of the putative functional roles and metabolic strategies of the dominant microbial taxa across the soil profile.

In the non-polluted sample SC1, large parts of the community grow chemolithotrophically to gain energy. In the heavily polluted and electron acceptor limited sample S4, microbial communities resort to methanogenesis and the potential transfer of excess electrons to neighbouring soil. Overall, the development of the microbial communities was mainly dependent on the combination of both PAH pollution (an oversupply of electrons) and the availability of electron acceptors. Microbial communities in samples SC3, SC4 and SC6 with limited electron acceptor availability were less diverse and unevenly distributed. In contrast, samples SC1, SC2 and SC5 with sufficient electron acceptors or absent PAH pollution, displayed greater diversity and community evenness. Translating these findings to natural attenuation suggests that we could take inspiration from these community responses. By adopting or enhancing the inherent microbial strategies used in the different environments, we can help overcome biodegradation-limiting factors.

3.7. *Microbial strategies observed across samples and feasible enhancements to improve bioremediation*

Firstly, the production or enabling of additional electron acceptors, which was seen in the form of the sulphate or iron reducing bacteria (*Thiobacillus, Desulfurivibrionaceae, Sulfurospirillaceae*). This method is already widely implemented in the field and involves the addition of electron acceptors, such as oxygen or sulphate (Dhar et al., 2020; Patel et al., 2020). An indirect, low-cost alternative to adding exogenous electron acceptors which we also observed in our results, is the fluctuation of groundwater levels, which enables the recycling of electron acceptors such as Fe^{3+}/Fe^{2+} or Mn^{4+}/Mn^{2+} upon oxygen exposure (Salowsky et al., 2021). This process was observed in sample SC2, where iron accumulation due to reoxidation above the groundwater level was found to provide sufficient electron acceptors for degradation. Therefore

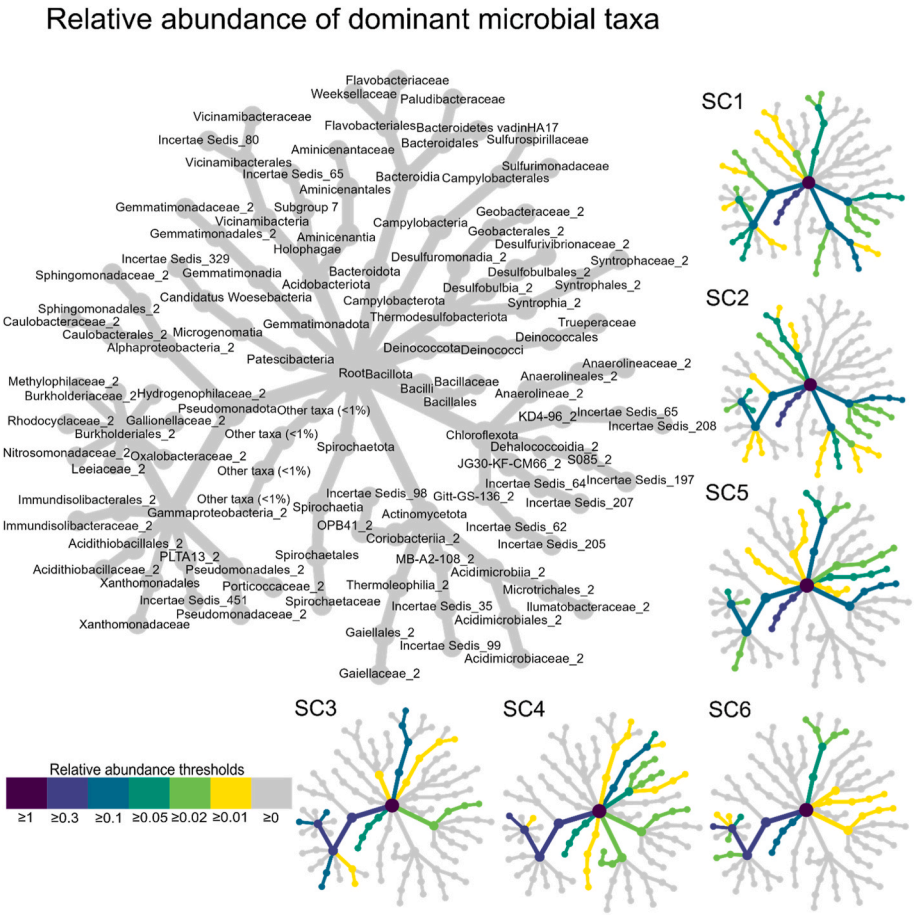

Fig. 3. Beta diversity and differential abundance analysis: Metacoder tree illustrating the dominant bacterial families across samples. The guide tree shows taxon names across different phylogenetic levels (Filtered min read count = 5, and present in at least 3 samples. Then filter out all <1% relative abundance at a family taxonomic level and group them under 'Other taxa'). The smaller embedded trees represent the dominant bacterial families in individual samples, based on averaged relative abundances per sample. The colour scale indicates relative abundance thresholds. (For interpretation of the references to colour in this figure legend, the reader is referred to the Web version of this article.)

Table 1
Summary of putative functional roles and metabolic strategies of dominant microbial taxa across the soil profile.

Soil sample	Taxonomic Identity	Putative Functional Role & Proposed Mechanism	Key Reference (s)
SC1	*Acidithiobacillaceae* (family)	**Iron/Sulphur Oxidation:** Chemolithoautotrophic metabolic pathways utilizing Fe^{2+} or elemental S^0.	(Gleisner et al., 2006; Quatrini and Johnson, 2019)
SC1	*Burkholderiales* (order) *Massilia* (genus)	**Aerobic PAH Degradation:** Primary colonizers of PAH-contaminated environments with ability to mineralize phenanthrene.	Wang et al. (2016)
SC1, SC2	*Acidimicrobiaceae* (family)	**Feammox:** Associated with Feammox process: oxidation of ammonium coupled to the reduction of iron under anaerobic/acidic conditions.	Huang et al. (2016)
SC1 and SC2	*Oxalobacteraceae* (family) *Massilia* (genus)	**Phytoremediation Support:** Linked to aerobic PAH degradation and pollutant uptake enhancement in the rhizosphere.	Amirhosseini et al. (2025)
SC1, SC2	*Chloroflexota KD4-96* (order)	**Soil Health Indicator:** Strongly correlated with high soil respiration rates and active carbon turnover in complex soil matrices.	Wilhelm et al. (2023)
SC1 and SC2	*Vicinamibacterales* (order)	**Phosphorus Cycling:** Chemoheterotrophs linked to phosphate solubilization phosphorus-availability.	(Huber and Overmann, 2018; Wu et al., 2022; Xia et al., 2023)
SC1, SC2, SC3, SC5	*Xanthomonadaceae* (family)	**PAH Degradation & Biosurfactants:** Production of biosurfactants to increase PAH bioavailability; potential holders of ring-hydroxylating dioxygenases.	(Lu et al., 2019; Sarkar et al., 2016)
SC2	*Actinomycetota MB-A2-108* (order)	**Soil Health Indicator:** Strongly correlated with high soil respiration rates and active carbon turnover in complex soil matrices.	Wilhelm et al. (2023)
SC2, SC3, SC4, SC6	*Hydrogenophillaceace* (family) *Thiobacillus* (genus)	**Sulphur/Iron Oxidation:** Oxidation of reduced sulphur (H_2S, S^0, pyrite) and Fe^{2+} to produce SO_4^{2-} and Fe^{3+}.	(Fortin et al., 1996; Harahuc et al., 2000; Quatrini and Johnson, 2019)
SC3	*Flavobacteriaceae* (family) *Lutibacter* (genus)	**Metabolic Flexibility:** Potentially capable of Hydrogenogenic fermentation; energy acquisition via H_2 oxidation; high Fe^{2+} tolerance. Habitat generalists and highly metabolically flexible	(Alharbi et al., 2026; Chen et al., 2021; Kessler et al., 2019)
SC3, SC6	*Rhodocyclaceae* (family) *Rugosibacter* (genus)	**Facultative aerobe PAH Degradation:** Capable of aromatic degradation under fluctuating oxygen levels; includes niche specialists for hypoxic conditions.	(Corteselli et al., 2017b; Sperfeld et al., 2018)
SC3, SC4, SC5, SC6	*Anaerolineaceae* (family)	**Primary Anaerobic Degradation:** Fermentation of complex organic matter/PAHs; potentially provides acetate and H_2 to methanogens.	(Bovio-Winkler et al., 2021; Lu et al., 2022)
SC4	*Sulfurspirillaceae* (family)	**Versatile Anaerobic Respiration:** Potential use of S^0, SO_4^{2-} or O_2 to oxidise organic acids/hydrogen.	(Finster et al., 1997; Ross et al., 2016)
SC4	*Geobacteraceae* (family)	**EET & Syntrophy:** Linked to extracellular electron transfer (EET); can act as iron-reducing partner for Anaerolineaceae in PAH-degrading consortia.	(Botton et al., 2007; Weber et al., 2006)
SC4	*Desulfurivibrionaceae* (family)	**Interspecies Electron Transfer:** Sulphate- and iron-reducing bacteria capable of EET; potentially facilitate long-distance electron transport.	(Chen et al., 2025; Su et al., 2023)
SC4, SC5	*Thermodesulfobacteriota* (class)	**Cable Bacteria-like Role:** Phylogenetically related to cable bacteria which indicates potential for long-distance electron transport toward zones with higher electron acceptor availability.	(Kjeldsen et al., 2019; Pfeffer et al., 2012)
SC4, SC6	*Methylophilaceae* (family)	**C1 Metabolism & HMW PAH degradation**: Utilization of methanol/methylated compounds; potentially degrading methylated HMW PAHs which accumulate in aged pollution.	(Chistoserdova, 2011; Lu et al., 2019; Salcher et al., 2019; Taubert et al., 2019)
SC5, SC6	*Weeksellaceae* (family) *Chryseobacterium* (genus)	**PAH degradation:** Associated with crude oil and PAH degradation.	(Márquez-Villa et al., 2023; Oberoi et al., 2015)
SC1, SC5	*Burkholderiaceae* (family)	**Aromatic compound degradation/High-Flux Electron Handling:** Associated with aromatic compounds degradation; Capacity to manage large electron supplies; documented occurrence at microbial fuel cell cathodes.	(Morya et al., 2020; Pimviriyakul et al., 2020; Simeon et al., 2022)
SC5, SC6	*Trueperaceae* (family)	**High-Flux Electron Handling:** Capacity to manage large electron supplies; documented occurrence at microbial fuel cell cathodes.	Simeon et al. (2022)
SC4, SC5	*Syntrophaceae* (family)	**Methanogenic Partner:** Partner in the syntrophic breakdown of complex carbon with methanogens; methanogenesis as terminal electron sink.	Walker et al. (2020)
SC5	*Gallionellaceae* (family)	**Iron Oxidation & CO_2 Fixation**: Fe^{2+} oxidation and autotrophic carbon fixation; might act as an alternative electron sink.	(Hallbeck and Pedersen, 1991; Huang et al., 2022)

(*continued on next page*)

Table 1 (*continued*)

Soil sample	Taxonomic Identity	Putative Functional Role & Proposed Mechanism	Key Reference (s)
SC5, SC6	*Bacteroidetes vadin HA17* (family)	**Methanogenic Conditions**: Associated with the degradation of complex organic matter alongside methanogenic partners.	Wei et al. (2019)
SC6	*Immundisolibacteraceae* (family)	**HMW PAH Degradation:** Specialized family reported for the degradation of high molecular-weight polycyclic aromatic hydrocarbons.	Corteselli et al. (2017a)

increasing groundwater level fluctuations frequency using low-cost methods like plant-mediated groundwater extraction using phreatophytes such as *Populus* or *Salix* could help re-oxidise previously utilized electron acceptors (Di et al., 2018).

A second strategy we observed was the potentially facilitated transport of electrons via cable bacteria related taxa (*Thermodesulfobacteriota*) from highly reducing zones into more oxidising zones. We observed a high abundance of *Thermodesulfobacteriota* in sample SC4 indicates ongoing interspecies electron transfer in this sample. This in combination with the presence of *Burkholderiaceae* and *Trueperaceae* —two families typically found at the cathode side of microbial fuel cells (Simeon et al., 2022) — in the neighbouring sample SC5, suggesting that SC5 could serve as an electron sink. Taken together, this indicates a potential dissemination of electrons throughout the soil. This brings us to an additional concept which could be used to improve biodegradation in heavily reducing environments, which is to facilitate the transport of electrons throughout the soil. This mechanism has been shown to enhance biodegradation in marine sediments through the development of an "oil-spill snorkel" linking filamentous *Desulfobulbaceae* with a conductive graphite rod, creating an electron bridge between anoxic and oxic zones (Matturro et al., 2017). Similarly, adding conductive pyrogenic carbon to peatland soils has been found to induce electron snorkeling, suppress methane production, and redirect electrons to a broader pool of electron acceptors (Sun et al., 2021).

A third strategy or concept emerging from this study is that when sufficient electron acceptors and PAH-degrading microorganisms are present, biodegradation can still be limited by other factors. In this study, this was observed due to the presence of phosphate-scavenging *Vicinamibacterales* in polluted sample SC2, where phosphorus limitation likely restricted growth and degradation. This limitation can be addressed in the field by supplementing phosphorus or by optimizing pH levels enhancing phosphorus availability and uptake, thereby restoring key microbial functions. The main takeaway is that, beyond redox balance, other limiting nutrients (nitrogen, phosphorus) and environmental factors (pH, temperature, bioavailability of pollutant) should also be optimized to enhance biodegradation.

Ultimately, our findings highlight the critical importance of monitoring microbial communities alongside standard assessments of redox conditions. This study demonstrates that even proximate samples can exhibit vastly different microbial needs depending on their access to pollutants and the local redox environment. Despite the limitations of this spatial gradient approach which provides only a static snapshot and cannot fully capture the intricate temporal dynamics, seasonal fluctuations and plume kinetics, we were able to successfully resolves the immediate localised constraints under true field conditions. Improving remediation efforts and the implementation of future low-cost solutions requires understanding microbial community needs. This will enable the supplementation of limiting factors or the proactive creation of conditions that minimize the constraints on biodegradation. While we recognise the inherent limitations in DNA-based monitoring, such as the presence of 'relic' DNA and the difficulty of inferring function from taxonomic information. Improving our understanding of the microbial community is vital for developing our understanding of these complex biogeochemical processes. Notably, our *in situ* observations are in strong alignment with recent subsurface simulation column experiments that tracked the responses of microbial communities before and after water table fluctuations in hydrocarbon-polluted soils (Xia et al., 2025). Their work provides valuable experimental evidence that water table dynamics are responsible for the active transport and replenishment of limiting electron acceptors. They even indicated that groundwater table fluctuations can function as a 'switch' within the local microbial communities, shifting between aerobic and anaerobic degradation (Xia et al., 2025). Specifically, they found that dissolved oxygen, nitrate, sulphate, and organic carbon concentrations serve as the primary drivers of temporal variation in bacterial community structure. Complementing these controlled lab-scale observations, our field-scale approach highlights how a clear, integrated physicochemical and microbial analysis can help guide future remediation strategies, such as inducing groundwater fluctuations, adding electron 'snorkels', or applying amendments to ensure sufficient nutrient and electron acceptor availability.

4. Conclusion

Despite the widespread reliance on natural attenuation for remediating petroleum-polluted soils, the process often remains slow and inefficient due to the complex interplay of microbial, physicochemical, and environmental factors. This study demonstrates that integrating physicochemical and biological analyses of PAH-polluted samples provides valuable insights regarding the mechanisms that restrict biodegradation. The findings presented here can inform broader applications aimed at enhancing biological remediation strategies. Moreover, analysing microbial communities offers a promising path toward more targeted and effective bioremediation, by addressing the key limitations constraining biodegradation as revealed through community responses associated with the conditions at hand.

CRediT authorship contribution statement

Simon Vandersanden: Writing – review & editing, Writing – original draft, Visualization, Software, Methodology, Investigation, Formal analysis, Data curation, Conceptualization. **Johan van Leeuwen:** Writing – review & editing, Supervision, Resources, Methodology, Investigation, Funding acquisition, Formal analysis, Conceptualization. **Jaco Vangronsveld:** Writing – review & editing, Supervision, Methodology, Funding acquisition. **Sofie Thijs:** Writing – review & editing, Supervision, Software, Resources, Methodology, Funding acquisition, Conceptualization.

Declaration of generative AI and AI-assisted technologies in the manuscript preparation process

During the preparation of this work the author(s) used ChatGPT in order to improve quality of the English writing. After using this tool/service, the author(s) reviewed and edited the content as needed and take(s) full responsibility for the content of the published article.

Funding

This study was financially supported by the EU-MIBIREM project funded by the European Union (Grant agreement ID: 101059260).

Declaration of competing interest

The authors declare the following financial interests/personal relationships which may be considered as potential competing interests:

Simon Vandersanden reports financial support was provided by European Union. If there are other authors, they declare that they have no known competing financial interests or personal relationships that could have appeared to influence the work reported in this paper.

Acknowledgments

The authors would like to thank Arie van Lit for providing detailed site information.

Appendix A. Supplementary data

Supplementary data to this article can be found online at https://doi.org/10.1016/j.envpol.2026.128559.

Data availability

Information with regard to raw sequencing data and soil parameter measurements can be found in the supplementary information.

References

Abdel-Shafy, H.I., Mansour, M.S.M., 2016. A review on polycyclic aromatic hydrocarbons: source, environmental impact, effect on human health and remediation. Egypt. J. Pet. 25, 107–123. https://doi.org/10.1016/j.ejpe.2015.03.011.

Alharbi, M., Nguyen-Dinh, T., Wong, W.W., Leung, P.M., Kessler, A.J., Greening, C., Cook, P.L.M., 2026. Dissimilatory nitrate reduction to ammonium driven by iron tolerant Lutibacter in coastal sediments. Sci. Total Environ. 1010, 181095. https://doi.org/10.1016/j.scitotenv.2025.181095.

Amirhosseini, K., Alizadeh, M., Azarbad, H., 2025. Harnessing the ecological and genomic adaptability of the bacterial genus massilia for environmental and industrial applications. Microb. Biotechnol. 18, e70156. https://doi.org/10.1111/1751-7915.70156.

Anneser, B., Einsiedl, F., Meckenstock, R.U., Richters, L., Wisotzky, F., Griebler, C., 2008. High-resolution monitoring of biogeochemical gradients in a tar oil-contaminated aquifer. Appl. Geochem. 23, 1715–1730. https://doi.org/10.1016/j.apgeochem.2008.02.003.

Botton, S., Van Harmelen, M., Braster, M., Parsons, J.R., Röling, W.F.M., 2007. Dominance of Geobacteraceae in BTX-degrading enrichments from an iron-reducing aquifer. FEMS (Fed. Eur. Microbiol. Soc.) Microbiol. Ecol. 62, 118–130. https://doi.org/10.1111/j.1574-6941.2007.00371.x.

Bovio-Winkler, P., Cabezas, A., Etchebehere, C., 2021. Database mining to unravel the ecology of the phylum chloroflexi in methanogenic full scale bioreactors. Front. Microbiol. 11. https://doi.org/10.3389/fmicb.2020.603234.

Callahan, B.J., McMurdie, P.J., Rosen, M.J., Han, A.W., Johnson, A.J.A., Holmes, S.P., 2016. DADA2: high-resolution sample inference from illumina amplicon data. Nat. Methods 13, 581–583. https://doi.org/10.1038/nmeth.3869.

Chen, S.-C., Li, X.-M., Battisti, N., Guan, G., Montoya, M.A., Osvatic, J., Pjevac, P., Pollak, S., Richter, A., Schintlmeister, A., Wanek, W., Mussmann, M., Loy, A., 2025. Microbial iron oxide respiration coupled to sulfide oxidation. Nature 646, 925–933. https://doi.org/10.1038/s41586-025-09467-0.

Chen, Y.-J., Leung, P.M., Wood, J.L., Bay, S.K., Hugenholtz, P., Kessler, A.J., Shelley, G., Waite, D.W., Franks, A.E., Cook, P.L.M., Greening, C., 2021. Metabolic flexibility allows bacterial habitat generalists to become dominant in a frequently disturbed ecosystem. ISME J. 15, 2986–3004. https://doi.org/10.1038/s41396-021-00988-w.

Chettri, D., Verma, A.K., Chirania, M., Verma, A.K., 2024. Metagenomic approaches in bioremediation of environmental pollutants. Environ. Pollut. 363, 125297. https://doi.org/10.1016/j.envpol.2024.125297.

Chistoserdova, L., 2011. Modularity of methylotrophy, revisited. Environ. Microbiol. 13, 2603–2622. https://doi.org/10.1111/j.1462-2920.2011.02464.x.

Cook, F., Knight, J., 2015. Where does oxygen extinction occur in a soil profile? 21st International Congress on Modelling and Simulation. Gold Coast, Australia.

Corteselli, E.M., Aitken, M.D., Singleton, D.R., 2017a. Description of Immundisolibacter cernigliae gen. nov., sp. Nov., a high-molecular-weight polycyclic aromatic hydrocarbon-degrading bacterium within the class Gammaproteobacteria, and proposal of Immundisolibacterales ord. nov. and Immundisolibacteraceae fam. nov. Int. J. Syst. Evol. Microbiol. 67, 925–931. https://doi.org/10.1099/ijsem.0.001714.

Corteselli, E.M., Aitken, M.D., Singleton, D.R., 2017b. Rugosibacter aromaticivorans gen. nov., sp. Nov., a bacterium within the family Rhodocyclaceae, isolated from contaminated soil, capable of degrading aromatic compounds. Int. J. Syst. Evol. Microbiol. 67, 311–318. https://doi.org/10.1099/ijsem.0.001714.

Davis, G.B., Patterson, B.M., Trefry, M.G., 2009. Evidence for instantaneous oxygen-limited biodegradation of petroleum hydrocarbon vapors in the subsurface. Groundwater Monitoring & Remediation 29, 126–137. https://doi.org/10.1111/j.1745-6592.2008.01221.x.

Davis, N.M., Proctor, D.M., Holmes, S.P., Relman, D.A., Callahan, B.J., 2018. Simple statistical identification and removal of contaminant sequences in marker-gene and metagenomics data. Microbiome 6, 226. https://doi.org/10.1186/s40168-018-0605-2.

Demin, K.A., Prazdnova, E.V., Minkina, T.M., Gorovtsov, A.V., 2024. Sulfate-reducing bacteria unearthed: ecological functions of the diverse prokaryotic group in terrestrial environments. Appl. Environ. Microbiol. 90, e0139023. https://doi.org/10.1128/aem.01390-23.

Dhar, K., Subashchandrabose, S.R., Venkateswarlu, K., Krishnan, K., Megharaj, M., 2020. Anaerobic Microbial Degradation of Polycyclic Aromatic Hydrocarbons: a Comprehensive Review, Reviews of Environmental Contamination and Toxicology, vol. 251. Springer International Publishing, Cham, pp. 25–108.

Di, N., Liu, Y., Mead, D.J., Xie, Y., Jia, L., Xi, B., 2018. Root-system characteristics of plantation-grown Populus tomentosa adapted to seasonal fluctuation in the groundwater table. Trees (Berl.) 32, 137–149. https://doi.org/10.1007/s00468-017-1619-2.

Dyksma, S., Pester, M., 2024. Growth of sulfate-reducing desulfobacterota and Bacillota at periodic oxygen stress of 50% air-O(2) saturation. Microbiome 12, 191. https://doi.org/10.1186/s40168-024-01909-7.

Faber, S.C., 2023. Field Investigations and Reactive Transport Modelling of Biodegrading Coal Tar Compounds at a Complex Former Manufactured Gas Plant. Utrecht University, Place. PhD Thesis.

Falih, K.T., Mohd Razali, S.F., Abdul Maulud, K.N., Abd Rahman, N., Abba, S.I., Yaseen, Z.M., 2024. Assessment of petroleum contamination in soil, water, and atmosphere: a comprehensive review. Int. J. Environ. Sci. Technol. 21, 8803–8832. https://doi.org/10.1007/s13762-024-05622-8.

Farnsworth, C.E., Voegelin, A., Hering, J.G., 2012. Manganese oxidation induced by water table fluctuations in a sand column. Environ. Sci. Technol. 46, 277–284. https://doi.org/10.1021/es2027828.

Finster, K., Liesack, W., Tindall, B.J., 1997. Sulfurospirillum arcachonense sp. Nov., a new microaerophilic sulfur-reducing bacterium. Int. J. Syst. Evol. Microbiol. 47, 1212–1217. https://doi.org/10.1099/00207713-47-4-1212.

Fortin, D., Davis, B., Beveridge, T.J., 1996. Role of Thiobacillus and sulfate-reducing bacteria in iron biocycling in oxic and acidic mine tailings. FEMS (Fed. Eur. Microbiol. Soc.) Microbiol. Ecol. 21, 11–24. https://doi.org/10.1111/j.1574-6941.1996.tb00329.x.

Gleisner, M., Herbert, R.B., Frogner Kockum, P.C., 2006. Pyrite oxidation by Acidithiobacillus ferrooxidans at various concentrations of dissolved oxygen. Chem. Geol. 225, 16–29. https://doi.org/10.1016/j.chemgeo.2005.07.020.

Gonzalez, V., Abarca-Hurtado, J., Arancibia, A., Claverías, F., Guevara, M.R., Orellana, R., 2024. Novel insights on extracellular electron transfer networks in the Desulfovibrionaceae family: unveiling the potential significance of horizontal gene transfer. Microorganisms 12, 1796. https://doi.org/10.3390/microorganisms12091796.

Hallbeck, L., Pedersen, K., 1991. Autotrophic and mixotrophic growth of Gallionella ferruginea. Microbiology 137, 2657–2661. https://doi.org/10.1099/00221287-137-11-2657.

Harahuc, L., Lizama, H.M., Suzuki, I., 2000. Selective inhibition of the oxidation of ferrous iron or sulfur in Thiobacillus ferrooxidans. Appl. Environ. Microbiol. 66, 1031–1037. https://doi.org/10.1128/aem.66.3.1031-1037.2000.

Harmsen, J., Rietra, R.P.J.J., 2018. 25 years monitoring of PAHs and petroleum hydrocarbons biodegradation in soil. Chemosphere 207, 229–238. https://doi.org/10.1016/j.chemosphere.2018.05.043.

Huang, S., Chen, C., Peng, X., Jaffé, P.R., 2016. Environmental factors affecting the presence of Acidimicrobiaceae and ammonium removal under iron-reducing conditions in soil environments. Soil Biol. Biochem. 98, 148–158. https://doi.org/10.1016/j.soilbio.2016.04.012.

Huang, Y.-M., Jakus, N., Straub, D., Konstantinidis, K.T., Blackwell, N., Kappler, A., Kleindienst, S., 2022. 'Candidatus ferrigenium straubiae' sp. nov., 'Candidatus ferrigenium bremense' sp. nov., 'Candidatus ferrigenium altingense' sp. Nov., are autotrophic Fe(II)-oxidizing bacteria of the family Gallionellaceae. Syst. Appl. Microbiol. 45, 126306. https://doi.org/10.1016/j.syapm.2022.126306.

Huber, K.J., Overmann, J., 2018. Vicinamibacteraceae fam. nov., the first described family within the subdivision 6 Acidobacteria. Int. J. Syst. Evol. Microbiol. 68, 2331–2334. https://doi.org/10.1099/ijsem.0.002841.

Hyland, C., 2006. Phosphorus Basics - the Phosphorus Cycle.

Kebede, G., Tafese, T., Abda, E.M., Kamaraj, M., Assefa, F., 2021. Factors influencing the bacterial bioremediation of hydrocarbon contaminants in the soil: mechanisms and impacts. J. Chem. 2021, 9823362. https://doi.org/10.1155/2021/9823362.

Kessler, A.J., Chen, Y.-J., Waite, D.W., Hutchinson, T., Koh, S., Popa, M.E., Beardall, J., Hugenholtz, P., Cook, P.L.M., Greening, C., 2019. Bacterial fermentation and respiration processes are uncoupled in anoxic permeable sediments. Nat. Microbiol. 4, 1014–1023. https://doi.org/10.1038/s41564-019-0391-z.

Kjeldsen, K.U., Schreiber, L., Thorup, C.A., Boesen, T., Bjerg, J.T., Yang, T., Dueholm, M. S., Larsen, S., Risgaard-Petersen, N., Nierychlo, M., Schmid, M., Bøggild, A., van de Vossenberg, J., Geelhoed, J.S., Meysman, F.J.R., Wagner, M., Nielsen, P.H., Nielsen, L.P., Schramm, A., 2019. On the evolution and physiology of cable bacteria. Proc. Natl. Acad. Sci. U. S. A. 116, 19116–19125. https://doi.org/10.1073/pnas.1903514116.

Kour, D., Kaur, T., Devi, R., Yadav, A., Singh, M., Joshi, D., Singh, J., Suyal, D.C., Kumar, A., Rajput, V.D., Yadav, A.N., Singh, K., Singh, J., Sayyed, R.Z., Arora, N.K., Saxena, A.K., 2021. Beneficial microbiomes for bioremediation of diverse contaminated environments for environmental sustainability: present status and future challenges. Environ. Sci. Pollut. Res. Int. 28, 24917–24939. https://doi.org/10.1007/s11356-021-13252-7.

Ley, P., Geelhoed, J.S., Vasquez-Cardenas, D., Meysman, F.J.R., 2024. On the diversity, phylogeny and biogeography of cable bacteria. Front. Microbiol. 15. https://doi.org/10.3389/fmicb.2024.1485281.

Lu, C., Hong, Y., Liu, J., Gao, Y., Ma, Z., Yang, B., Ling, W., Waigi, M.G., 2019. A PAH-degrading bacterial community enriched with contaminated agricultural soil and its utility for microbial bioremediation. Environ. Pollut. 251, 773–782. https://doi.org/10.1016/j.envpol.2019.05.044.

Lu, J., Guo, Z., Pan, Y., Li, M., Chen, X., He, M., Wu, H., Zhang, J., 2022. Simultaneously enhanced removal of PAHs and nitrogen driven by Fe2+/Fe3+ cycle in constructed wetland through automatic tidal operation. Water Res. 215, 118232. https://doi.org/10.1016/j.watres.2022.118232.

Márquez-Villa, J.M., Rodríguez-Sierra, J.C., Amtanus Chequer, N., Cob-Calan, N.N., García-Maldonado, J.Q., Cadena, S., Hernández-Núñez, E., 2023. Phenanthrene degradation by photosynthetic bacterial consortium dominated by Fischerella sp. Life 13. https://doi.org/10.3390/life13051108.

Matturro, B., Cruz Viggi, C., Aulenta, F., Rossetti, S., 2017. Cable bacteria and the bioelectrochemical snorkel: the natural and engineered facets playing a role in hydrocarbons degradation in marine sediments. Front. Microbiol. 8, 952. https://doi.org/10.3389/fmicb.2017.00952.

Meckenstock, R.U., Boll, M., Mouttaki, H., Koelschbach, J.S., Cunha Tarouco, P., Weyrauch, P., Dong, X., Himmelberg, A.M., 2016. Anaerobic degradation of Benzene and polycyclic aromatic hydrocarbons. J. Mol. Microbiol. Biotechnol. 26, 92–118. https://doi.org/10.1159/000441358.

Meckenstock, R.U., Elsner, M., Griebler, C., Lueders, T., Stumpp, C., Aamand, J., Agathos, S.N., Albrechtsen, H.-J., Bastiaens, L., Bjerg, P.L., Boon, N., Dejonghe, W., Huang, W.E., Schmidt, S.I., Smolders, E., Sørensen, S.R., Springael, D., van Breukelen, B.M., 2015. Biodegradation: updating the concepts of control for microbial cleanup in contaminated aquifers. Environ. Sci. Technol. 49, 7073–7081. https://doi.org/10.1021/acs.est.5b00715.

Mekonnen, B.A., Aragaw, T.A., Genet, M.B., 2024. Bioremediation of petroleum hydrocarbon contaminated soil: a review on principles, degradation mechanisms, and advancements. Front. Environ. Sci. 12. https://doi.org/10.3389/fenvs.2024.1354422.

Mohapatra, B., Phale, P.S., 2021. Microbial degradation of naphthalene and substituted naphthalenes: metabolic diversity and genomic insight for bioremediation. Front. Bioeng. Biotechnol. 9. https://doi.org/10.3389/fbioe.2021.602445.

Morya, R., Salvachúa, D., Thakur, I.S., 2020. Burkholderia: an untapped but promising bacterial genus for the conversion of aromatic compounds. Trends Biotechnol. 38, 963–975. https://doi.org/10.1016/j.tibtech.2020.02.008.

Murali, A., Bhargava, A., Wright, E.S., 2018. IDTAXA: a novel approach for accurate taxonomic classification of microbiome sequences. Microbiome 6, 140. https://doi.org/10.1186/s40168-018-0521-5.

Oberoi, A.S., Philip, L., Bhallamudi, S.M., 2015. Biodegradation of various aromatic compounds by enriched bacterial cultures: part A–Monocyclic and polycyclic aromatic hydrocarbons. Appl. Biochem. Biotechnol. 176, 1870–1888. https://doi.org/10.1007/s12010-015-1684-1.

Ohmura, N., Matsumoto, N., Sasaki, K., Nagaoka, T., Saiki, H., 1999. Growth of Thiobacillus ferrooxidans on hydrogen by the dissimilatory reduction of ferric iron under anaerobic conditions. In: Amils, R., Ballester, A. (Eds.), Process Metallurgy. Elsevier, pp. 767–775.

OVAM, 2025. Compendium voor monsterneming en analyses van afvalstoffen en bodem (CMA). https://emis.vito.be/nl/erkende-laboratoria/bodem-en-afvalstoffen-ovam/compendium-cma.

Patel, A.B., Shaikh, S., Jain, K.R., Desai, C., Madamwar, D., 2020. Polycyclic aromatic hydrocarbons: sources, toxicity, and remediation approaches. Front. Microbiol. 11, 562813. https://doi.org/10.3389/fmicb.2020.562813.

Penn, C.J., Camberato, J.J., 2019. A critical review on soil chemical processes that control how soil pH affects phosphorus availability to plants. Agriculture 9, 120.

Pfeffer, C., Larsen, S., Song, J., Dong, M., Besenbacher, F., Meyer, R.L., Kjeldsen, K.U., Schreiber, L., Gorby, Y.A., El-Naggar, M.Y., Leung, K.M., Schramm, A., Risgaard-Petersen, N., Nielsen, L.P., 2012. Filamentous bacteria transport electrons over centimetre distances. Nature 491, 218–221. https://doi.org/10.1038/nature11586.

Pimviriyakul, P., Wongnate, T., Tinikul, R., Chaiyen, P., 2020. Microbial degradation of halogenated aromatics: molecular mechanisms and enzymatic reactions. Microb. Biotechnol. 13, 67–86. https://doi.org/10.1111/1751-7915.13488.

Quatrini, R., Johnson, D.B., 2019. Acidithiobacillus ferrooxidans. Trends Microbiol. 27, 282–283. https://doi.org/10.1016/j.tim.2018.11.009.

Roden, E.E., 2003. Fe(III) oxide reactivity toward biological versus chemical reduction. Environ. Sci. Technol. 37, 1319–1324. https://doi.org/10.1021/es026038o.

Ross, D.E., Marshall, C.W., May, H.D., Norman, R.S., 2016. Comparative genomic analysis of Sulfurospirillum cavolei MES reconstructed from the metagenome of an electrosynthetic microbiome. PLoS One 11, e0151214. https://doi.org/10.1371/journal.pone.0151214.

Salcher, M.M., Schaefle, D., Kaspar, M., Neuenschwander, S.M., Ghai, R., 2019. Evolution in action: habitat transition from sediment to the pelagial leads to genome streamlining in Methylophilaceae. ISME J. 13, 2764–2777. https://doi.org/10.1038/s41396-019-0471-3.

Salowsky, H., Schäfer, W., Schneider, A.-L., Müller, A., Dreher, C., Tiehm, A., 2021. Beneficial effects of dynamic groundwater flow and redox conditions on natural attenuation of mono-, poly-, and NSO-heterocyclic hydrocarbons. J. Contam. Hydrol. 243, 103883. https://doi.org/10.1016/j.jconhyd.2021.103883.

Santos, M., Rebola, S., Evtuguin, D.V., 2025. Soil remediation: current approaches and emerging bio-based trends. Soil Syst. 9, 35. https://doi.org/10.3390/soilsystems9020035.

Sarkar, J., Kazy, S.K., Gupta, A., Dutta, A., Mohapatra, B., Roy, A., Bera, P., Mitra, A., Sar, P., 2016. Biostimulation of Indigenous microbial community for bioremediation of petroleum refinery sludge. Front. Microbiol. 7, 1407. https://doi.org/10.3389/fmicb.2016.01407.

Simeon, I.M., Weig, A., Freitag, R., 2022. Optimization of soil microbial fuel cell for sustainable bio-electricity production: combined effects of electrode material, electrode spacing, and substrate feeding frequency on power generation and microbial community diversity. Biotechnol. Biofuels Bioprod. 15, 124. https://doi.org/10.1186/s13068-022-02224-9.

Sperfeld, M., Diekert, G., Studenik, S., 2018. Anaerobic aromatic compound degradation in Sulfuritalea hydrogenivorans sk43H. FEMS (Fed. Eur. Microbiol. Soc.) Microbiol. Ecol. 95. https://doi.org/10.1093/femsec/fiy199.

Su, K., Li, L., Wang, Q., Cao, R., 2023. A review on the interspecies electron transfer of methane production in anaerobic digestion system. Fermentation 9, 467. https://doi.org/10.3390/fermentation9050467.

Sun, T., Guzman, J.J.L., Seward, J.D., Enders, A., Yavitt, J.B., Lehmann, J., Angenent, L. T., 2021. Suppressing peatland methane production by electron snorkeling through pyrogenic carbon in controlled laboratory incubations. Nat. Commun. 12, 4119. https://doi.org/10.1038/s41467-021-24350-y.

Taubert, M., Grob, C., Crombie, A., Howat, A.M., Burns, O.J., Weber, M., Lott, C., Kaster, A.K., Vollmers, J., Jehmlich, N., von Bergen, M., Chen, Y., Murrell, J.C., 2019. Communal metabolism by Methylococcaceae and Methylophilaceae is driving rapid aerobic methane oxidation in sediments of a shallow seep near Elba, Italy. Environ. Microbiol. 21, 3780–3795. https://doi.org/10.1111/1462-2920.14728.

van Beek, C.G.E.M., Cirkel, D.G., de Jonge, M.J., Hartog, N., 2021. Concentration of Iron (II) in fresh groundwater controlled by siderite, field evidence. Aquat. Geochem. 27, 49–61. https://doi.org/10.1007/s10498-020-09390-y.

Walker, D.J.F., Nevin, K.P., Holmes, D.E., Rotaru, A.-E., Ward, J.E., Woodard, T.L., Zhu, J., Ueki, T., Nonnenmann, S.S., McInerney, M.J., Lovley, D.R., 2020. Syntrophus conductive pili demonstrate that common hydrogen-donating syntrophs can have a direct electron transfer option. ISME J. 14, 837–846. https://doi.org/10.1038/s41396-019-0575-9.

Walters, W., Hyde, E.R., Berg-Lyons, D., Ackermann, G., Humphrey, G., Parada, A., Gilbert, J.A., Jansson, J.K., Caporaso, J.G., Fuhrman, J.A., Apprill, A., Knight, R., 2016. Improved bacterial 16S rRNA gene (V4 and V4-5) and fungal internal transcribed spacer marker gene primers for microbial community surveys. mSystems 1. https://doi.org/10.1128/mSystems.00009-15.

Wang, H., Lou, J., Gu, H., Luo, X., Yang, L., Wu, L., Liu, Y., Wu, J., Xu, J., 2016. Efficient biodegradation of phenanthrene by a novel strain Massilia sp. WF1 isolated from a PAH-contaminated soil. Environ. Sci. Pollut. Control Ser. 23, 13378–13388. https://doi.org/10.1007/s11356-016-6515-6.

Weber, K.A., Achenbach, L.A., Coates, J.D., 2006. Microorganisms pumping iron: anaerobic microbial iron oxidation and reduction. Nat. Rev. Microbiol. 4, 752–764. https://doi.org/10.1038/nrmicro1490.

Weelink, S.A., van Doesburg, W., Saia, F.T., Rijpstra, W.I., Röling, W.F., Smidt, H., Stams, A.J., 2009. A strictly anaerobic betaproteobacterium Georgfuchsia toluolica gen. nov., sp. Nov. degrades aromatic compounds with Fe(III), Mn(IV) or nitrate as an electron acceptor. FEMS Microbiol. Ecol. 70, 575–585. https://doi.org/10.1111/j.1574-6941.2009.00778.x.

Wei, J., Gao, J., Wang, N., Liu, Y., Wang, Y., Bai, Z., Zhuang, X., Zhuang, G., 2019. Differences in soil microbial response to anthropogenic disturbances in Sanjiang and Momoge Wetlands, China. FEMS (Fed. Eur. Microbiol. Soc.) Microbiol. Ecol. 95. https://doi.org/10.1093/femsec/fiz110.

Wilhelm, R.C., Amsili, J.P., Kurtz, K.S.M., van Es, H.M., Buckley, D.H., 2023. Ecological insights into soil health according to the genomic traits and environment-wide associations of bacteria in agricultural soils. ISME Commun. 3, 1. https://doi.org/10.1038/s43705-022-00209-1.

Wu, X., Rensing, C., Han, D., Xiao, K.Q., Dai, Y., Tang, Z., Liesack, W., Peng, J., Cui, Z., Zhang, F., 2022. Genome-resolved metagenomics reveals distinct phosphorus acquisition strategies between soil microbiomes. mSystems 7, e0110721. https://doi.org/10.1128/msystems.01107-21.

Xia, M., Ma, X., Liu, J., Wu, M., Li, Z., Liu, M., 2023. Potential effect of key soil bacterial taxa on the increase of rice yield under milk vetch rotation. Front. Microbiol. 14. https://doi.org/10.3389/fmicb.2023.1150505.

Xia, X., Jia, W., Wang, K., Ding, A., 2025. Seasonal distribution of microbial community and n-Alkane functional genes in diesel-contaminated groundwater: influence of water table fluctuation. Water 17, 1710.

Xu, F., Li, P., He, Q., Ning, J., Li, X., 2025. Experimental insights into iron and manganese transformation in soil during groundwater fluctuations. J. Contam. Hydrol. 275, 104677. https://doi.org/10.1016/j.jconhyd.2025.104677.